A PRELIMINARY ANALYTIC EVALUATION OF THE SEISMIC RESPONSE OF STRUCTURAL WALLS FAILING IN A SHEAR MODE

L. M. Robinson*

ABSTRACT

This study examines the role of inelastic shear deformations in attenuating response of structural walls subjected to seismic excitation. Particular emphasis is placed on required shear strength having regard to damage potential, usable ductilities, and strength erosion. First the load-deformation relations for reinforced concrete structural walls failing in shear are discussed and simplified modelling of these relations introduced. Previous analytic studies using this simplified modelling and artificial earthquake simulation are then reviewed. This present study uses similar procedures to those previously employed, but with real earthquake accelerograms, and a modelling refined to account for strength erosion. It is demonstrated through simple concepts correlated by time history analyses that existing code provisions may be unnecessarily conservative in many applications.

1. INTRODUCTION

The New Zealand Standard NZS 4203 [1] requires that structures be designed to resist an equivalent lateral seismic load V given by

$$V = C_d W_t \qquad (1)$$

where C_d, the design seismic coefficient is

$$C_d = CSMR \qquad (2)$$

in which: C is the basic seismic coefficient, dependent on geographic location; S is the structural type factor; M is the factor for the material of construction; and R is a risk factor reflecting the importance of the building to the community or the consequences of failure.

For reinforced concrete or reinforced masonry structures the product SM equal to 4 is assigned for structures not specifically detailed for fully ductile or limited ductile response. Such structures are expected to respond to earthquake excitation without significant yielding of reinforcement. Structures of limited ductility, however, are assigned a structural type factor of S = 2, with M = 0.8 for reinforced concrete and M = 1.0 for reinforced masonry. Such limited ductile structures are required to be suitably designed and detailed to preclude premature shear failure.

To meet the requirement for precluding shear failure, the materials codes NZS 3101 [2] for reinforced concrete, and NZS 4230 [3] for reinforced masonry, require that members possess a shear strength with a suitable margin above their flexural strength. This is attained by providing that the ideal shear strength, V_i, of each member b[illegible]rived from

$$\phi V_i \geq \lambda V_{eq} + V_g \qquad (3)$$

where: ϕ is the strength reduction factor; V_{eq} is the shear force in the member on the application of the lateral loads specified in Eq. (1) and with SM = 1.6 or 2.0 for reinforced concrete and reinforced masonry, respectively; and V_g is the appropriately factored shear force in the member due to gravity loads. Recognising that V_g is likely to be insignificant in comparison with V_{ew}, in structural walls, Eq. (3) reduces to

$$\phi V_i \geq \lambda V_{eq} \qquad (4)$$

where λ is the strength enhancement factor and is not to be taken as less than 2.0. Thus the required shear strength is not less than that associated with assumed elastic response for reinforced masonry (SM = 4.0) and close to this same level for reinforced concrete (SM = 3.2), assuming redistribution of design actions is not employed. In calculating the strength, only one-half of the contribution of the masonry or concrete which would normally be assumed under gravity load conditions may be assumed, in recognition of the erosion of this mechanism of resistance due to flexural yielding and associated cracking.

The purpose of these rules is to inhibit shear failure, since the response of structures failing in a shear mode is not well understood, and therefore reliance on such mechanisms for attenuating seismic response is considered inadvisable. The Code provisions follow the suggestions of the Study Group of the New Zealand National Society for Earthquake Engineering [4]. Originally that group considered means of reducing the demands in special cases, notably in squat shear walls, but, while recognising that shear failure modes may be acceptable in many instances, the approach was abandoned in the interests of overall simplicity. But the achievement of the stated objective through the simplified

* Consulting Engineer, Dunedin.

formulation can produce onerous demands, particularly in meeting the limitations of total shear stress applying in the materials codes to control diagonal compression.

For example, it may be shown, using the provisions outlined above for reinforced masonry, the maximum shear specified for Grade B masonry, and common building masses, that the gross cross-sectional area of masonry is about 2 percent of the building plan area per storey of construction. This is difficult to incorporate into contemporary building forms.

It is toward reviewing these current provisions that this paper is addressed. While the discussion will focus on reinforced concrete structural walls, the content remains largely applicable to reinforced masonry structural walls.

2. SHEAR FORCE-DISPLACEMENT RELATION

Experiments conducted on squat shear walls, in which flexural deformations are small, designed to fail in shear, demonstrate that the envelope of cyclic load-deflection plots approximate the load-deflection curve obtained for monotonic loading. Barda [5], for instance, reports this phenomenon, common in many engineering materials, from experiments conducted on walls tested principally monotonically but including selective, though limited, cyclic testing.

A typical behaviour is shown in Fig. 1(a). For the positive quadrant envelope, which is the load-deflection curve derived from monotonic loading, the following points are observed. After cracking shear, V_{cr}, has been reached, there is a sudden loss of tangent stiffness which continues to reduce as the load is increased through the point at which web steel begins to yield to the point at which the maximum achievable strength, V_{max}, is attained. Between V_{cr} and V_{max} the mean stiffness is greatly reduced below the original tangent stiffness, typically by as much as 90 percent. At V_{max} the shear deflections in the walls have increased by an order of magnitude above those at V_{cr}. Further deformation leads to reducing strength and the associated tangent stiffness is negative. At displacements in the order of 40 times those at cracking the shear strength has eroded to that provided by the shear reinforcement alone, V_s.

For the case of loads applied by gravity, the attainment of V_{max} signals complete failure in almost all structures because shedding of shear actions is difficult to achieve in most structures loaded by gravity loads. Shear failure has thus, correctly, been ascribed as brittle, and a condition to be avoided. However, where the loading is deformation controlled, attainment of V_{max} signals only a reduction of member reaction under further deformation. In this sense the behaviour may be described as ductile. There is a fundamental difference between behaviour which is load-controlled and that which is deformation-controlled. This may be seen in that $\Delta \neq \Delta(V)$ is not single valued, in general, but the inverse relation $V = V(\Delta)$ is usually single-valued. Earthquake loading is similar in nature to deformation-controlled behaviour.

It is apparent,then, that advantage might be taken of the relatively ductile behaviour of shear deformations, and the resulting limiting of earthquake induced actions. Furthermore, significant softening of the shear stiffness will lead to increased period and, usually, a reduction of response.

Fig. 1(a) indicates typical cyclic load-deflection paths, bounded largely by the monotonic envelope. Experimental data on the nature of these paths is scarce, so that adequate mathematical modelling for numeric time history analyses is difficult to achieve. A useful approximation is the Origin-Oriented model, due to Umemura [6]. This approximation is shown in Fig. 1(b). Several deficiencies are to be noted. Since each path passes through the origin, no residual deflections on unloading are possible, contrary to experimental evidence. Further, experiments show that there will be considerable lag on reloading (even monotonically) so that deflections are required to exceed those in all previous cycles in order to achieve actions equal to or greater than those achieved in the previous cycles. These phenomena are similar to the slack which builds up in cross-braced frames in which the braces yield only in tension: the parallel here is that shear cracks must close before diagonal compression can develop across them. Nevertheless, use of these assumptions in the modelling is believed to be conservative. Principal concern over the use of the modelling is with the apparent neglect of the strength degradation for deformations beyond those at V_{max}.

3. PREVIOUS STUDIES

It has been expressed by several writers that a principal objective in earthquake resistant design is the achievement of large load-deflection loops, so that significant energy is dissipated by hysteresis. It is known that variation of the shape of the loops has little influence on the response, and there is growing evidence [7,8] that the area within the loops is of less consequence than was thought to be the case. Of greater importance, it seems, is the actual maximum achievable displacement, provided that strength degradation is not too severe. These considerations lend confidence in the use of shear failure modes as an acceptable means of attenuating seismic response.

Analytical studies attempting to model the behaviour of structural walls failing in a shear mode have been conducted. Murakami and Penzien [9] used the simplified Origin-Oriented model of Umermura, which does not take account of the falling branch of the load-deflection curve, and studied the response of such systems to filtered white noise using time intensity functions to model several, each of various earthquake types. Figure 2 is drawn from their

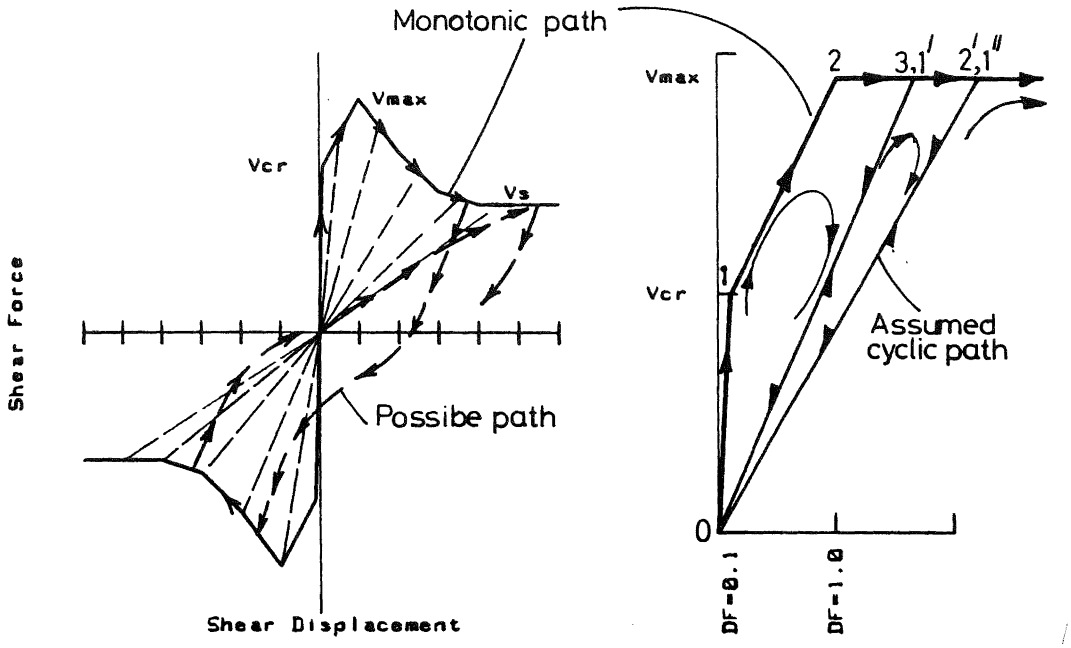

Fig 1 SHEAR FORCE - DISPLACEMENT RELATIONS FOR SHEAR-FAILING SYSTEMS

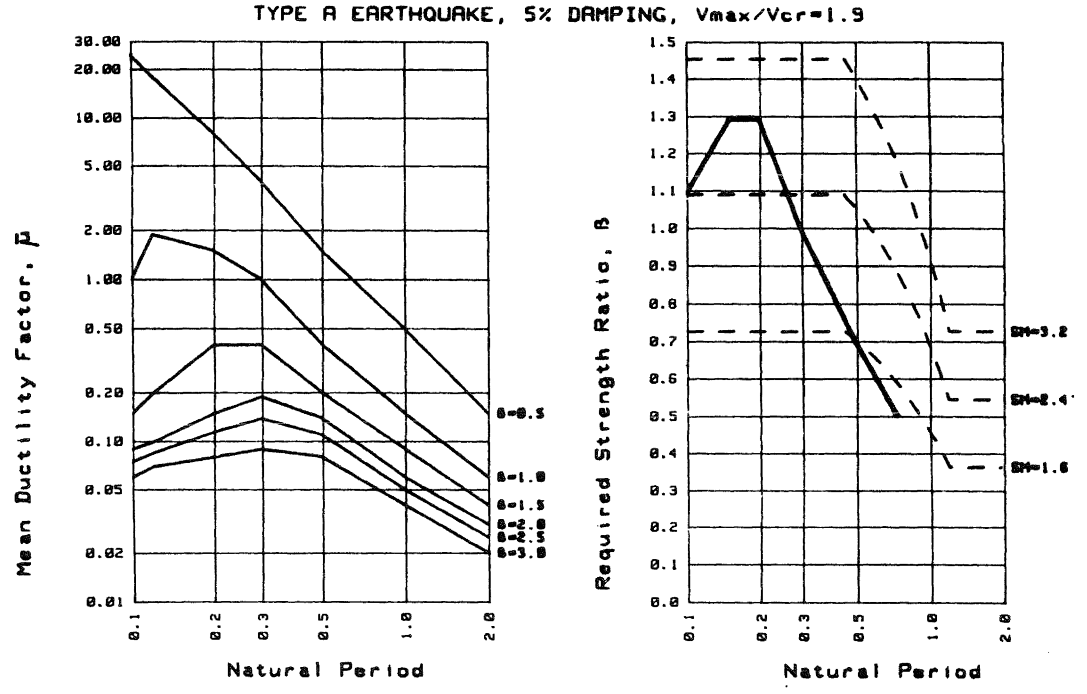

Fig 2 RESPONSE OF ORIGIN-ORIENTED SHEAR MODEL SUBJECTED TO ARTIFICIAL EARTHQUAKE RECORDS (AFTER MURAKAMI AND PENZIEN)

results for Type A earthquakes, those of greatest duration. Figure 2(a) shows the mean ductility factor, related to the deflection at V_{max} in Fig. 1(b) as unity, required for varying strength ratios, β, plotted against the natural period of vibration. The term "ductility factor" as used here and in [9] is not what is customarily understood by the term. A more descriptive terminology would be "shear strain ratio", relating the shear strain at the point of interest to some reference point. But in spite of the imprecise language, use of the more familiar term "ductility factor" will be continued. To avoid confusion, a subscript v will be added so that μ_v is the shear ductility factor understood to mean a shear-strain ratio. In their study Murakami and Penzien use the strain at cracking as the reference strain. It seems more natural to use the strain at the attainment of V_{max} as the reference point, and their results have been adjusted accordingly. Note that in their studies, shear deformation is implied as being the total deformation, a point which is taken up later in discussing their results. The strength ratio is defined as $V_{max}/m\ddot{x}_g$, where m is the mass of the single-mass system studied, and $\ddot{x}_g$ is the peak ground acceleration.

Because there is considerable scatter in the results, a ductility factor corresponding to a higher confidence level than the mean is more meaningful.

For the selected confidence level a non-linear response spectrum can be drawn. In deriving the spectrum an appropriate level of ductility factor must be selected. Umemura has suggested 1.0 as an appropriate level for controlling damage in extreme earthquakes, and 0.2 for controlling damage in more frequent events, defined as those having maximum ground accelerations of two-thirds the extreme event. The former case tends to control for short-period structures, the latter controlling for long-period structures. These criteria were adopted by Murakami and Penzien.

Figure 2(b), after Murakami and Penzien, is a response spectrum for a shear ductility factor of 1.0 at the 85 percent probability distribution level. Assuming a peak ground acceleration of 0.33g to be appropriate for New Zealand seismic Zone A, as defined in NZS 4203, the spectra for given SM products can be shown on the same graph. It is seen that SM = 3.2, as currently specified in NZS 3101 is appropriate for short period structures - and for longer period structures if the second Umemura criterion is also adopted.

The following factors should be taken into accout in studying analytical results such as those reported above.

(a) Ductility factors greatly in excess of unity employing the Origin-Oriented model of Fig. 1(b) should be disregarded, since the falling branch of Fig. 1(a) is not accounted for. This does not invalidate Fig. 2(b), which employs for its basis a ductility factor of unity.

(b) A ductility factor of unity is rather small for an extreme event. Barda achieved ductility factors in the order of 40 before there was serious disintegration of squat walls. However, inelastic flexural cracking could reduce the attainable levels.

(c) The structures studied were single mass systems. Shear failure at levels other than the base in multi-mass systems excite the higher modes of vibration which have significantly altered characteristics of response.

(d) The load-deflection relation shown in Fig. 1(b) will only be approximately true for the structure as a whole where the height of the inelastic shear zone is a significant fraction of the total height of the wall. Thus walls with larger aspect ratio can be expected to behave quite differently from those of small aspect ratio.

4. FORMULATION AND MODELLING EMPLOYED IN THIS STUDY

The paucity of data relating to shear failing systems precludes the use of sophisticated mathematical modelling or analytical techniques. Even under laboratory control, the variation in strength and stiffness is large in nominally identical walls. Reinforced concrete, taken to extensive cracking, is very difficult to model - even displacement continuity is lost across cracks and iterative procedures to redistribute force imbalance at cracking are costly. The following, however, are thought appropriate in this preliminary study.

4.1 Selection of Shear Ductility Factor

In selecting the shear ductility factor, recognition must be made of the strength erosion resulting. NZS 4203 comments that individual elements of ductile structures should not lose more than 30 percent of their strength when cycled through eight load reversals to ductility factors of 4/SM. Clearly this is of principal concern if the full contribution of the concrete, V_c, is assumed for the shear strength. In that event a ductility factor of not more than 2.0 is appropriate. If only 50 percent of V_c is assumed, a ductility factor of 4.0 would be a maximum. However, where no contribution from the concrete is assumed, little strength erosion below V_s, the shear assigned to the steel, will be evident and the choice of the ductility factor will be dictated by consideration of damage alone, and the possible resulting loss of integrity in the wall. Then a ductility factor up to 10 is thought appropriate. It is to be expected that as the ductility factor increases, there will be a large difference between $|MAX(\mu_v)|$ and $|MIN(\mu_v)|$. Hence a ductility factor of 10 might imply, for certain earthquake disturbances, a maximum of $|\mu_v|$ of 20 or more, so that use of a maximum value of 10 is not unduly conservative. It is considered that the range of ductility,

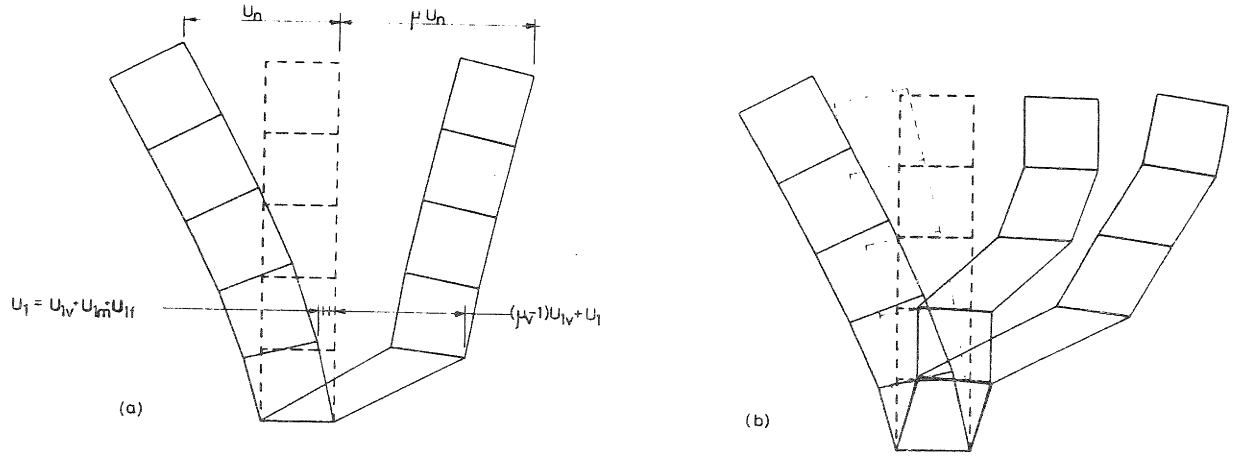

Fig 3 DISPLACEMENTS OF STRUCTURAL WALLS

(a) AS MODELLED IN THIS STUDY

(b) EXTREME DEFORMATIONS NOT CONSIDERED IN THIS STUDY

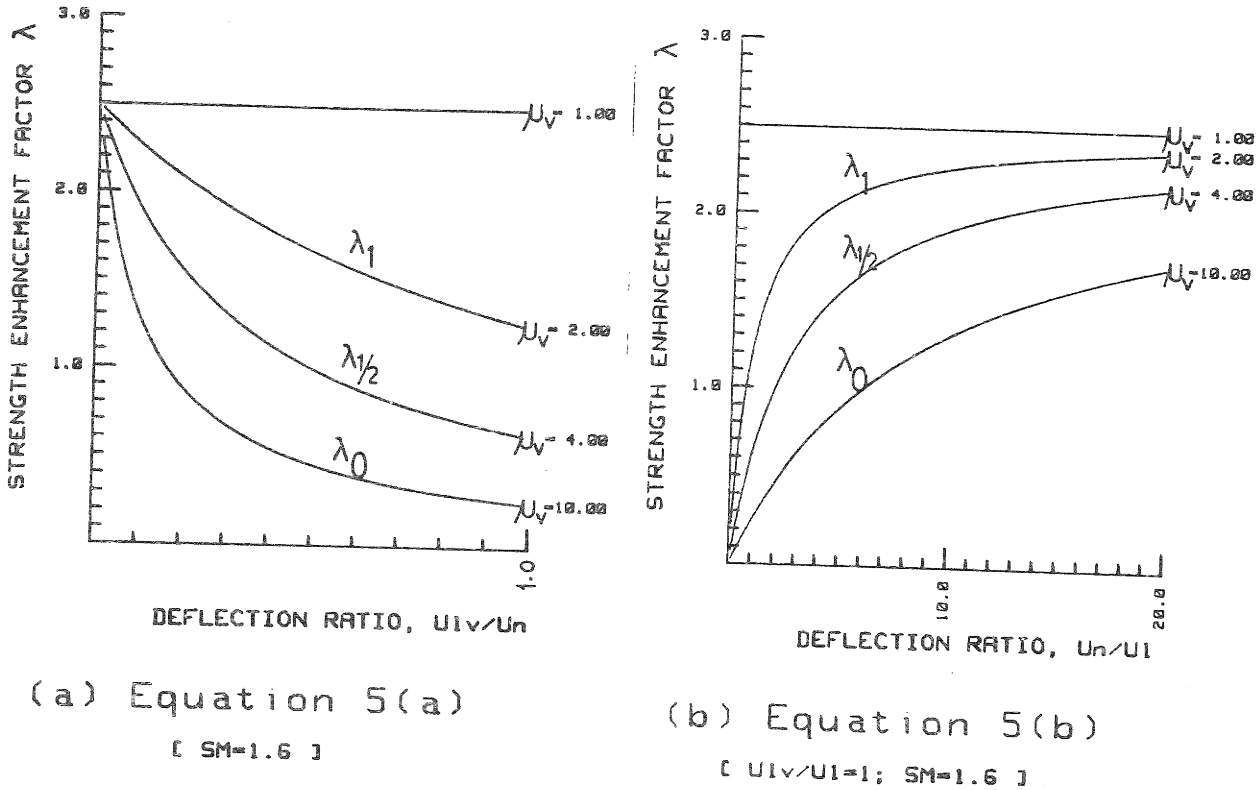

Fig 4 REQUIRED SHEAR STRENGTH ENHANCEMENT FACTOR AS A FUNCTION OF SHEAR DUCTILITY FACTORS AND DEFORMATION RATIOS

$|MAX(\mu_v)| + |MIN(\mu_v)|$, has relevance to damage, and the half-range value (equivalent to the numeric average) is intended by the control ductility of 2,4, or 10 nominated above.

4.2 Maximum Shear Stress

Experiments on squat walls designed to fail in shear [3] suggest that the maximum shear resistance is independent of the quantity of web reinforcement, vertical or horizontal, unless the steel ratio is very large. Flexural yielding, even partial, is however likely to influence this, and consequently the maximum ideal resistance, V_i, should not be assumed greater than $V_c + V_s$, as is customary, but with a maximum ideal shear stress of $0.2f'_c$. In addition the cracking shear, V_{cr}, should not be assumed greater than V_c.

4.3 Shear Force-Displacement Relationship

The Origin-Oriented model, modified to account for the falling branch, is an appropriate model to study the influence of shear stiffness and strength degradation. For walls in which flexural yielding is inhibited, the flexural stiffness is not greatly reduced below that obtained at first flexural cracking.

4.4 Influence of Wall Height

Figure 3(a) shows the deflection of an illustrative wall at code level load, defined as loads corresponding to SM = 1.6, and at a higher level of load at which shear failure in the bottom element has occurred. Extreme cases involving failure of elements further up the walls, such as is shown in Figure 3(b) are not considered here.

At code level load the deflection at the top of the bottom element is U_1, comprised of U_{1v}, due to shear, U_{1m}, due to flexure, and U_{1f} due to foundation rotation and associated effects. At this same level of load the top of the wall has deflected U_n due to all sources.

At greatest deformation the deflection at the top of the bottom element has increased. Assuming that this increase is occasioned entirely through shear deformation, and that there is no increase in shear beyond that at code level loading, the deflection is given by $U_1 + (\mu_v - 1)U_{1v}$, where μ_v is the shear ductility factor. The top of the wall has increased in deflection to μU_n, where μ is the overall displacement ductility factor required. Consistent with the assumption that inelastic deformation is due entirely to shear, then

$$(\mu - 1)U_n = (\mu_v - 1)U_{1v} \qquad (a)$$

Assuming now that μ is given by $4/SM\lambda$, where λ is a scalar to achieve enhanced shear strength, then

$$\left(\frac{4}{SM\lambda} - 1\right)U_n = (\mu_v - 1)U_{1v} \qquad (b)$$

Rearranging,

$$\lambda = \frac{4}{SM}\left\{\frac{1}{(\mu_v - 1)U_{1v}/U_n + 1}\right\} \qquad (5a)$$

$$= \frac{4}{SM}\left\{\frac{U_n/U_1}{(\mu_v - 1)U_{1v}/U_1 + U_n/U_1}\right\} \qquad (5b)$$

In Eq. (5b), the ratio U_n/U_1 is related to the aspect ratio of the wall, h_w/ℓ_w, where h_w is the height of the wall, and ℓ_w is its breadth. If ℓ_w is also taken as the height over which inelastic shear deformation is significant, than $U_n/U_1 = h_w/\ell_w$ for a linear deflection profile at code level loading. Eqs. (5a) and (5b) demonstrate the influence of wall aspect ratio and the relative contribution of shear deformation to total deformation in defining the likely magnitude of required strength enhancement to limit shear ductility, Eq. (5a) is graphed in Fig. (4a) and Eq. (5b) in Fig. (4b).

4.5 Modelling Employed

To test the responses of structural walls several walls were analysed under simulated earthquake loading. Of those studied eight are reported herein. Each wall is labelled uniquely thus

$$N_1L_1N_2$$

where: N_1 is the number of storeys in the structure; L_1 is a letter, "R" for a rectangular wall or "C" for a channel shaped wall; and N_2 is the number of hundreds of tonnes tributary mass per floor level.

In all cases the walls are 3 m wide and are of 200 mm thickness. To avoid the issue of the proper height of the wall which is subject to significant inelastic shear deformation, each storey height is assumed to be 3.0 m and this height is taken as the height of a wall element.

Each element of the wall is modelled as a beam element, and a lumped mass modelling employed.

In all cases the value of ϕV_{cr} and ϕV_c were taken as 550 kN, the dependable shear strength based on $\phi = 0.85$, a shear stress of $0.3\sqrt{f'_c}$, and an effective depth of $0.8\ell_w$.

Each wall was analysed for all modes of vibration based on uncracked gross section properties, and the first mode period, T_1, thus determined used to calculate V_{code} using the Zone A spectrum of NZS 4203. The dependable strength afforded by the steel, ϕV_s, was incremented by $0.5V_{code}$ from $0.5V_{code}$ to $3.0V_{code}$. V_{max} was assumed to be equal to $V_c + V_s$ in all cases, with all flexural yielding inhibited. For each value of V_s (6 per wall), each wall was subject to each of 4 different earthquake excitations.

The envelope for the force-deformation curves was constructed from limited experimental data and is, for the positive

TABLE 1 : WALL DETAILS

WALL	NUMBER OF STOREYS	SECTION SHAPE	MASS PER LEVEL (tonnes)	PERIOD (second)	V_{code} (kN)*	DEFLECTION (mm)		
						U_n	U_1	U_{1v}
1R2	1	Rectangle	200	0.119	471	0.77	0.77	0.29
1C2	1	Channel	200	0.087	471	0.44	0.44	0.29
1R4	1	Rectangle	400	0.168	942	1.53	1.53	0.59
1C4	1	Channel	400	0.123	942	0.87	0.87	0.59
2R1	2	Rectangle	100	0.209	471	3.39	1.24	0.29
2C1	2	Channel	100	0.131	471	1.36	0.58	0.29
3R1	3	Rectangle	100	0.395	706	14.33	2.56	0.44
3C1	3	Channel	100	0.234	706	5.02	1.08	0.44

*V_{code} is calculated for seismic zone A with S = 2, M = 0.8, and R = 1.0

TABLE 2 : COMPARISON OF RESULTS FROM NON-LINEAR TIME HISTORY ANALYSIS AND THE DETERMINISTIC APPROACH OF EQ. (5a)

WALL	PARAMETER	PF, SS, EC	SS,EC	Eq. (5a)
1R2	$\mu_v = 10 : \lambda_0$	0.6	(0.0)	0.56
	$\mu_v = 4 : \lambda_{\frac{1}{2}}$	1.3	0.7	1.16
	$\mu_v = 2 : \lambda_1$	2.0	1.5	1.81
1C2	$\mu_v = 10 : \lambda_0$	0.4	(0.0)	0.35
	$\mu_v = 4 : \lambda_{\frac{1}{2}}$	1.2	0.6	0.83
	$\mu_v = 2 : \lambda_1$	2.0	1.4	1.49
1R4	$\mu_v = 10 : \lambda_0$	1.1	0.3	0.56
	$\mu_v = 4 : \lambda_{\frac{1}{2}}$	1.6	1.0	1.16
	$\mu_v = 2 : \lambda_1$	2.0	1.9	1.81
1C4	$\mu_v = 10 : \lambda_0$	0.8	0.3	0.35
	$\mu_v = 4 : \lambda_{\frac{1}{2}}$	1.5	0.8	0.83
	$\mu_v = 2 : \lambda_1$	2.0	1.6	1.49
2R1	$\mu_v = 14 : \lambda_0$	0.6	0.1	1.40
	$\mu_v = 4 : \lambda_{\frac{1}{2}}$	1.3	1.0	1.98
	$\mu_v = 2 : \lambda_1$	2.1	1.9	2.30
2C1	$\mu_v = 10 : \lambda_0$	0.5	(0.0)	0.85
	$\mu_v = 4 : \lambda_{\frac{1}{2}}$	1.3	0.6	1.52
	$\mu_v = 2 : \lambda_1$	2.0	1.6	2.06
3R1	$\mu_v = 10 : \lambda_0$	2.1	0.6	1.96
	$\mu_v = 4 : \lambda_{\frac{1}{2}}$	3.2	1.6	2.29
	$\mu_v = 2 : \lambda_1$	4.0	2.3	2.43
3C1	$\mu_v = 10 : \lambda_0$	1.2	0.4	1.40
	$\mu_v = 4 : \lambda_{\frac{1}{2}}$	1.7	1.1	1.98
	$\mu_v = 2 : \lambda_1$	2.3	2.0	2.30

NOTE: PF = Parkfield, SS = Sinesweep, EC = El Centro
Bracketted figures extrapolated, to a non-negative value.

quadrant, as follows:

(a) For $\mu_v \leq 0.1$, the uncracked stiffness of the wall was assumed. V_{cr} occurs at the end of this interval.

(b) For $0.1 < \mu_v \leq 1$, a linear variation between V_{cr} and V_{max} was assumed.

(c) For $\mu_v > 1$, the ideal shear strength is given by $V_i = V_s + \eta V_c$ where

$$\eta = \mu_v^{k(1 - \mu_v)} \qquad (6)$$

The constant k was conservatively assumed to be unity.

The load-deformation paths bounded by the envelope were taken as in the Origin-Oriented model.

The choice of walls was such that the initial fundamental period was always less than 0.4s, typical of the period of walls of principal interest. Since the bases were assumed to be fully fixed, thus preventing energy feedback to the ground or dissipation through ground compliance, the results should be conservative.

Details of the walls are shown in Table 1.

4.6 Earthquake Simulation

Four different accelerograms were used:

- The N-S component of the 1940 El Centro event, the de facto standard.
- The Johnson/Epstein Sinesweep Earthquake [10]. This artificial record is a short duration analytic earthquake with a maximum acceleration level of 0.33g, and was developed as an equivalent to the El Centro 1940 N-S accelerogram. It may be viewed as a signal resulting from a deconvolution process of a prescribed signal at the foundation level.
- The Parkfield earthquake, of 1965.
- The first 7 seconds of the Pacoima Dam earthquake. This earthquake is a particularly severe event, and is thought to be inappropriate to a study of this type. The effect of its extreme nature was reduced by considering only the first 7 seconds, still vigorous, and this was included only as a control for extreme events.

The linear response spectra for 10 percent damping for each earthquake are shown in Fig. 5. Damping of 10 percent critical was employed throughout this study.

5. RESULTS OF SIMULATED EARTHQUAKE EXCITATION

The results of the nonlinear time history analyses are summarised in Fig. 6. These figures are drawn for μ_v against λ_0 where λ_0 is defined as

$$\lambda_0 = \frac{\phi V_s}{V_{code}} \qquad (7a)$$

Similarly, with obvious meaning attaching to the subscripts 0, ½, and 1, $\lambda_{½}$ and λ_1 are defined as

$$\lambda_{½} = \frac{\phi(V_s + ½V_c)}{V_{code}} \qquad (7b)$$

$$\lambda_1 = \frac{\phi(V_s + V_c)}{V_{code}} \qquad (7c)$$

As outlined previously μ_v is here interpreted as the half-range of ductilities, $(MAX(\mu_v) - MIN(\mu_v))/2$.

Clearly results for $\lambda_{½}$ and λ_1 can be derived by translating the λ_0 curves to the right by $½\phi V_c/V_{code}$ and $\phi V_c/V_{code}$ respectively. This has not been done in Fig. 6, to avoid clutter.

On each graph Eq. (5a) has been drawn as a dashed line, for reference.

Several observations can be made:

(a) The channel shaped walls generally require a smaller λ to control ductility demand. This is partly due to period reduction, but equally it is due to the reduction of flexural deformation.

(b) The ductility demand increases as the ratio V_{code}/V_c increases, pointing to a preference to keep design stresses at code level loading relatively small.

(c) As can be expected, the largest variable is the earthquake itself. Note, however, the close agreement between the El Centro and Sinesweep results, even in this non-linear study.

(d) There is significant variation between walls as to the controlling earthquake. For example for wall 3R1 Parkfield clearly controls, but for the stiffer 3C1 wall the short motion Pacoima earthquake controls. This can be explained by reference to the spectra and the period reduction from 0.395s for 3R1 to 0.234s for 3C1.

In general, however, the Pacoima earthquake controls, even with the reduced record employed. Otherwise Parkfield tends to control for $\lambda < 1.5$, with not a great variation between all earthquakes (excluding Pacoima) for greater values of λ.

Table 2 shows the results of the analyses for $\lambda_0, \lambda_{½}$ and λ_1 separately, and compares these values thus derived with those derived through Eq. (5a).

From Table 2 the following additional general observation can be made,

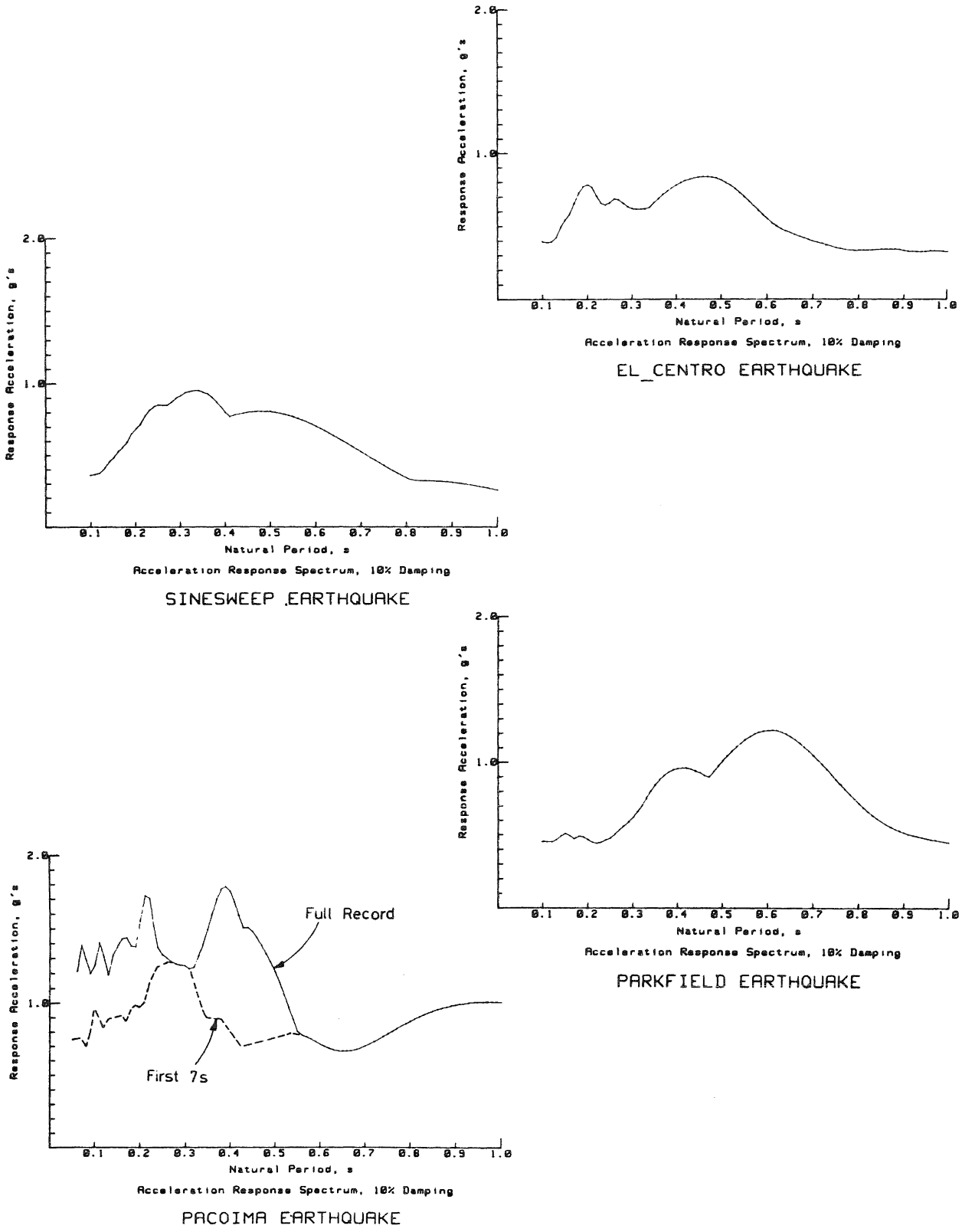

Fig 5 ACCELERATION RESPONSE SPECTRA FOR FOUR EARTHQUAKES AT 10 PER-CENT OF CRITICAL DAMPING

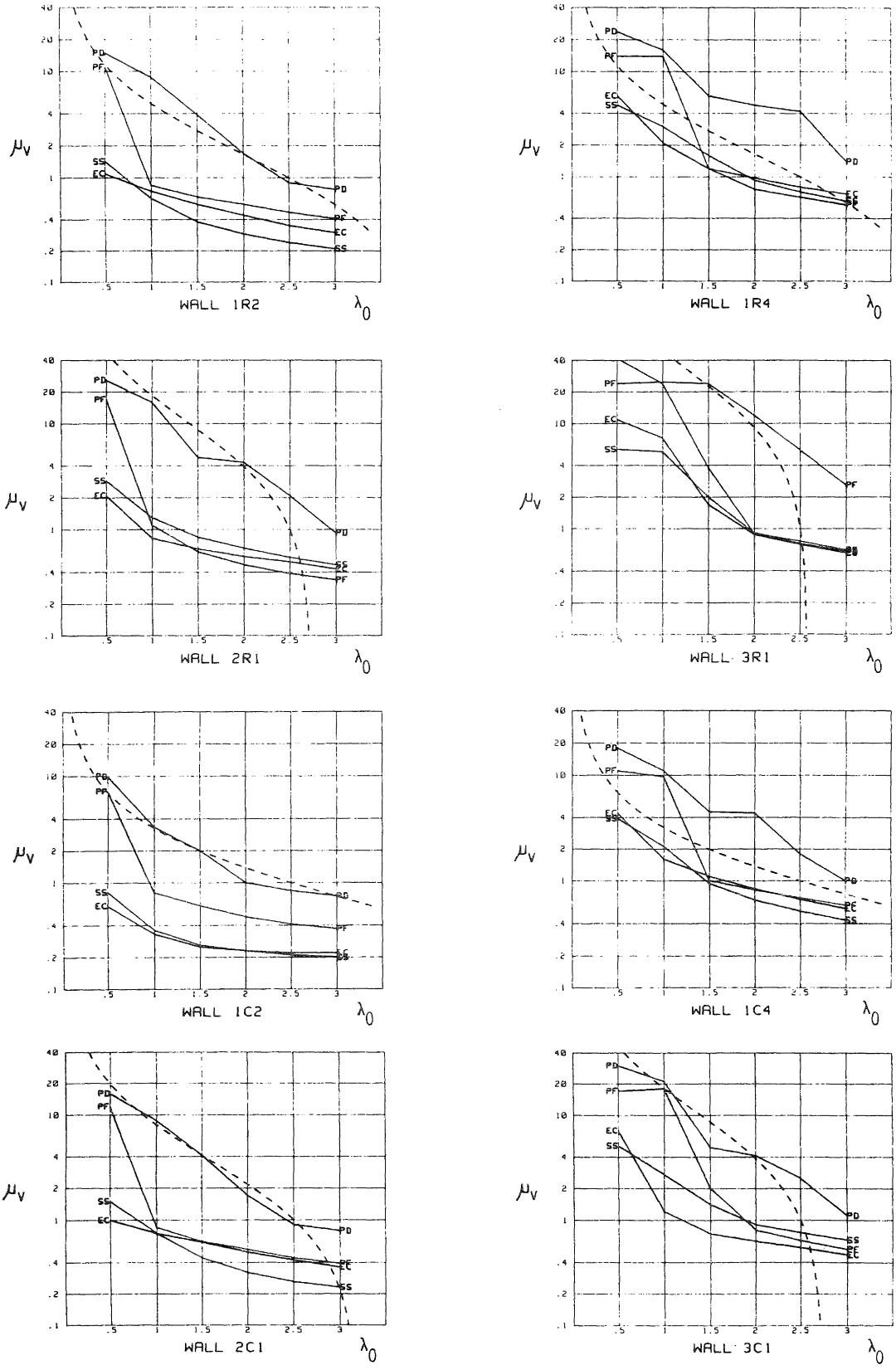

Fig 6 SHEAR DUCTILITY DEMAND PLOTTED AGAINST SHEAR STRENGTH ENHANCEMENT FACTOR FOR EIGHT WALL TYPES

TABLE 3 $T_1(\mu_v)$: FIRST MODE PERIOD OF VIBRATION AS A FUNCTION OF SHEAR DUCTILITY FACTOR, BASED ON $V_{cr} = V_c = V_s$ AND THE ORIGIN-ORIENTED SHEAR MODEL

WALL	$T_1(\mu_v)$, seconds				
	$\mu_v \leq 0.1$	$\mu_v = 1$	$\mu_v = 2$	$\mu_v = 4$	$\mu_v = 10$
1R2	0.119	0.182	0.277	0.453	0.708
1C2	0.087	0.164	0.267	0.447	0.707
1R4	0.168	0.258	0.392	0.640	1.002
1C4	0.123	0.232	0.378	0.632	1.000
2R1	0.209	0.245	0.318	0.477	0.723
2C1	0.131	0.188	0.281	0.455	0.709
3R1	0.395	0.422	0.483	0.644	0.923
3C1	0.234	0.282	0.377	0.576	0.881

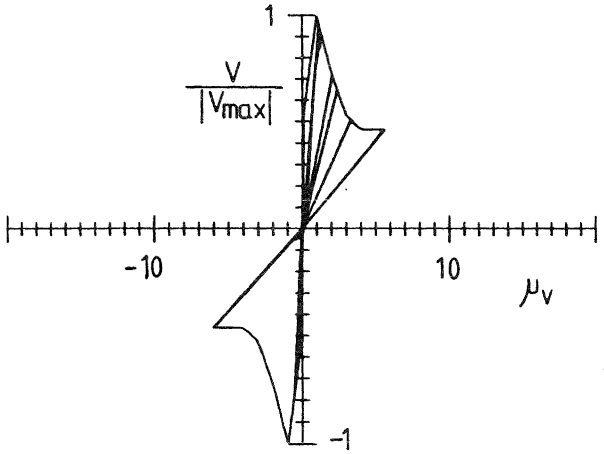

(a) WALL 1R4, EL CENTRO EARTHQUAKE

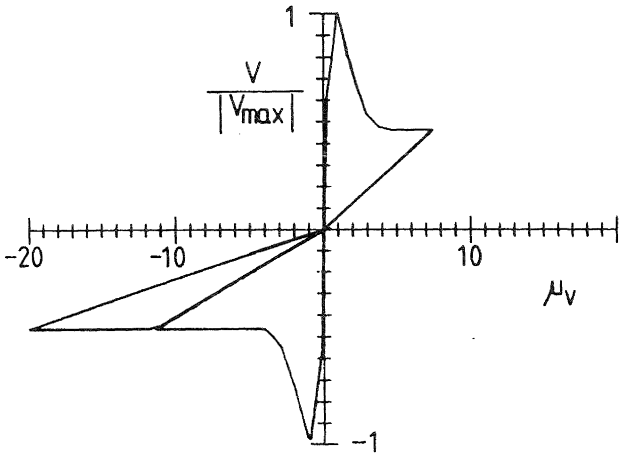

(b) WALL 1R4, PARKFIELD EARTHQUAKE

Fig 7 HYSTERETIC RESPONSE OF WALL 1R4 SUBJECTED TO EL CENTRO AND PARKFIELD ACCELEROGRAMS

(e) Eq. (5a) is unconservative when Parkfield is included in the analysis, but otherwise Eq. (5a) produces conservative results, with minor exceptions. The "equal displacement" hypothesis upon which Eqs. (5) are based is known to apply more closely to El Centro type motions, than to most others.

Figure 7 shows the hysteretic response diagrams for wall 1R4 for $\lambda_0 = \phi V_s/V_{code} = 0.5$ subject to the El Centro and Parkfield accelerograms. These hysteresis response diagrams are generally typical of response, and additional general observations can be made.

(f) Larger average ductilities are often associated with a large disparity between $|MAX(\mu_v)|$ and $|MIN(\mu_v)|$.

(g) Few excursions beyond the current maximum ductility are encountered. In this connection it appears that period adjustments are often sufficient to protect against further increases in the current maximum ductility factor in each direction.

A special property of the Origin-Oriented model is that if the maximum and minimum shear ductility factors are numerically equal and have both been reached, then the continuation of response of the system is linear (except for geometric non-linearities, usually insignificant in walls). We may therefore legitimately refer to periods of vibration unambiguously without reference to amplitude. Table 3 lists the first mode period of vibration for each wall as a function of the shear ductility factor, assumed reached in both directions in the bottom element. It is seen that the period shift is significant in all cases. Sometimes the shift is into a region of increased response (as in wall 3R1 for the Parkfield earthquake), but more often than not this shift is such as to produce response. In this connection it is conservative (often overly so) to use the shifted period and the original response spectrum. This is because the response spectrum is drawn for the maximum acceleration experienced by the system during the entire seismic excitation; but the response to cause the period shift is usually associated with an already significant elapsed time from the commencement of shaking. Procedures can be derived to allow such estimates, but this is beyond present purposes. In any event, the modelling employed is too crude to warrant such sophistication.

6. CONCLUSIONS

This investigation has studied the response of simple structural wall forms under earthquake attack. The study has not been comprehensive, choosing to concentrate attention on inelastic shear deformations and excluding such important topics as concurrent inelastic flexural deformation.

Within the limitations of the study it has been demonstrated that the existing code requirements for shear strength are conservative, often not overly so but equally often unduly so. The code tends to be too conservative for walls in which shear deformation is a significant source of total deformation, as is the case in squat walls. This has been demonstrated, and that the principal parameters to describe the required strength can be assembled into simple expressions using familiar concepts.

Once more the question of the role of ductility has been examined. It again appears that, provided the necessary displacements can be achieved without large strength erosion, areas of hysteresis loops need not be large.

Clearly more research, both experimental and analytic, needs to be undertaken to determine a more adequate shear force-displacement model, including the interactive effects of moment and shear, and such further information as is required for routine finite element analyses. Without such information mathematical modelling must of necessity be but very coarse and analytic results, such as those which do not include allowance for shear softening, viewed somewhat suspiciously.

7. REFERENCES

[1] NZS 4203:1984 "Code of Practice for the General Structural Design and Design Loadings for Buildings", Standards Association of New Zealand.

[2] NZS 3101:1982 "Code of Practice for the Design of Concrete Structures", Standards Association of New Zealand.

[3] NZS 4230:1985 "Code of Practice for the Design of Masonry Structures", Standards Association of New Zealand.

[4] Robinson, L.M., "Shear Walls of Limited Ductility", Bulletin of the New Zealand National Society for Earthquake Engineering, Vol. 13, No. 2, June 1980.

[5] Barda, F., "Shear Strength of Low Rise Walls with Boundary Elements", Ph.D. dissertation, Lehigh University, Bethlehem, Pennsylvania, U.S.A., 1972.

[6] Umemura, J., et al, "Earthquake Resistant Design of Reinforced Concrete Buildings, Accounting for the Dynamic Effects of Earthquakes", Giho-Do, Tokyo, Japan, 1973 (in Japanese).

[7] Dean, J.A., Stewart, W.G. and Carr, A.J., "The Seismic Behaviour of Plywood Sheathed Shearwalls", Bulletin of the New Zealand National Society for Earthquake Engineering, Vol. 19, No. 1, March 1986.

[8] Moss, P.J., Carr, A.J. and Buchanan, A.H., "Seismic Response of Low-Rise Buildings", Bulletin of the New Zealand National Society for Earthquake Engineering, Vol.19,No.3, Sept. 1986.

[9] Murakami, M. and Penzien, J., "Non-Linear Response Spectra for Probabilistic Seismic Design of Reinforced Concrete Structures", Seventh World Conference on Earthquake Engineering, Istanbul, 1980.

[10] Johnson, G.R. and Epstein, H.I., "Short Duration Analytic Earthquake", Journal ASCE, Structural Division, 102, No. ST5, 1976.

8. LIST OF SYMBOLS

C = basic seismic coefficient, geographic zone dependent.

C_d = design seismic coefficient

= CSMR

f'_c = compressive strength of concrete, MPa

$\sqrt{f'_c}$ = square root of f'_c, MPa

g = acceleration of gravity, 9.81 m/s^2

h_w = height of wall

k = numeric constant, assumed as unity

ℓ_w = horizontal length of wall in the plane of loading

m = mass of simple oscillator

M = material factor

R = risk factor

S = structural type factor

T_1 = $T_1(\mu_v)$ = first mode period of vibration

U_1 = total displacement through the bottom element at code level loading

U_{1f} = displacement through the bottom element due to foundation rotation and related effects at code level loading

U_{1v} = shear displacement through the bottom element at code level loading

U_n = total displacement at the top of the structure at code level loading

V = total design base shear, or general force

V_c = ideal shear strength provided by the concrete for $\mu_v = 1$

V_{code} = design base shear in the wall at code level loading

V_{cr} = cracking shear

V_{eq} = design earthquake shear in the element at code level loading

V_g = appropriately factored design gravity load shear in the element

V_i = ideal shear strength

V_{max} = maximum value of shear strength

V_s = ideal shear strength provided by the shear reinforcement

W_t = total seismic mass multiplied by g

= total seismic weight

$\ddot{x}_g$ = peak ground acceleration

β = $V_{max}/m\ddot{x}_g$

Δ = general deformation

η = $\eta(\mu_v)$ = ratio of shear resisted by the concrete at given μ_v, to V_c

λ = strength enhancement factor

λ_0 = $\phi V_s/V_{code}$

$\lambda_{\frac{1}{2}}$ = $\phi(V + \frac{1}{2}V_c)/V_{code}$

λ_1 = $\phi(V_s + V_c)/V_{code}$

μ = overall displacement ductility factor

μ_v = shear displacement ductility factor, the ratio of shear strain at given displacement to the shear strain at displacement corresponding to V_{max}

ϕ = strength reduction factor